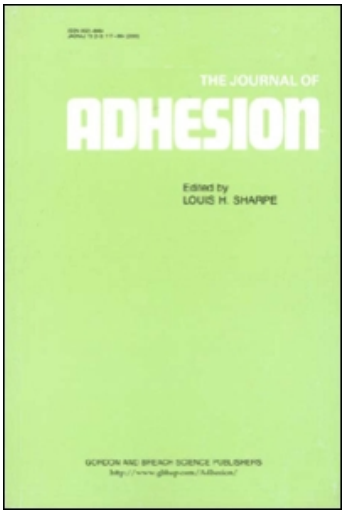

The Journal of Adhesion
Publication details, including instructions for authors and subscription information:
http://www.informaworld.com/smpp/title~content=t713453635

Characterization of Ambient Temperature Cure Epoxies Used in Adhesive Anchor Applications

Joannie Chin[a]; Aaron Forster[a]; Cyril Clerici[a]; Donald Hunston[a]
[a] Polymeric Materials Group, Materials and Construction Research Division, National Institute of Standards and Technology, Gaithersburg, Maryland, USA

Online publication date: 27 October 2010

To cite this Article Chin, Joannie , Forster, Aaron , Clerici, Cyril and Hunston, Donald(2010) 'Characterization of Ambient Temperature Cure Epoxies Used in Adhesive Anchor Applications', The Journal of Adhesion, 86: 10, 1041 — 1067
To link to this Article: DOI: 10.1080/00218464.2010.515494
URL: http://dx.doi.org/10.1080/00218464.2010.515494

The Journal of Adhesion, 86:1041–1067, 2010
ISSN: 0021-8464 print/1545-5823 online
DOI: 10.1080/00218464.2010.515494

Taylor & Francis
Taylor & Francis Group

Characterization of Ambient Temperature Cure Epoxies Used in Adhesive Anchor Applications

Joannie Chin, Aaron Forster, Cyril Clerici, and Donald Hunston
Polymeric Materials Group, Materials and Construction Research Division, National Institute of Standards and Technology, Gaithersburg, Maryland, USA

Thermo-viscoelastic properties of two commercial, ambient temperature-cure epoxy structural adhesives were analyzed and compared. The adhesives were formulated by the same manufacturer and appeared to have the same base chemistry; however, one system contained accelerators for shorter cure times. In the laboratory, dynamic mechanical temperature/frequency sweeps were performed on both systems to generate dynamic mechanical data and predict creep compliance master curves using frequency-temperature superposition principles. Differential scanning calorimetry (DSC), thermogravimetric analysis (TGA), and moisture sorption analysis were also used to assess the thermal and hygroscopic properties of the materials. Differences were observed in the thermal, hydrolytic, and dynamic mechanical properties of the two adhesive systems as well as in their estimated creep compliance behavior, which were attributed to differences in the curing agent(s) and accelerator(s) used in the adhesive systems. In most cases the differences in the properties of the epoxies were small, but a few properties, particularly the predicted creep behavior, exhibited very large differences. Results from laboratory creep testing confirmed the predicted difference in creep behavior. The data also suggest that dynamic mechanical testing combined with frequency-temperature superposition may be a useful metrology for predicting trends for in-service creep behavior from short term tests.

Keywords: Adhesive anchors; Adhesives; Creep compliance; Differential scanning calorimetry; Dynamic mechanical thermal analysis; Epoxy; Moisture sorption analysis; Thermogravimetric analysis; Time- or frequency-temperature superposition

Received 28 August 2009; in final form 1 July 2010.

One of a Collection of papers honoring David A. Dillard, the recipient in February 2010 of *The Adhesion Society Award for Excellence in Adhesion Science, Sponsored by 3M*.

Address correspondence to Joannie Chin, Materials and Construction Research Division, Building and Fire Research Laboratory, NIST, 100 Bureau Drive, Stop 8615, Gaithersburg, MD 20899, USA. E-mail: joannie.chin@nist.gov

INTRODUCTION

In building and construction applications, ambient temperature-cured structural adhesives are commonly used for bonding of threaded rod anchors and other inserts into cured concrete [1], bonding of steel or fiber composite reinforcing plates to bridge decks [2], and retrofitting of concrete columns [3]. These adhesives are two-component systems in which one component contains the base resin and the other component contains curing agents, catalysts, and/or accelerators. The base resin is commonly an epoxy, isophthalic polyester, or vinyl ester. Other ingredients used in the two components include flow control agents and/or inorganic fillers such as silica, titanium dioxide, or calcium carbonate.

The two components, usually contained in separate containers, are combined at the point of application. As soon as the resin and curing agent come in contact, curing is initiated and the viscosity of the mixture begins to rise rapidly through the formation of crosslink networks. Once the networks traverse the entire sample, *gelation* is said to have occurred [4]. With continued cure, the resin vitrifies and becomes a rigid, glassy structure. At this point, the molecular mobility of the material is so low that it is difficult for reactive groups to diffuse to each other and, thus, the curing process essentially stops. Vitrification of room temperature-cured thermosets can occur before all of the available groups have reacted; thus, such materials may not be fully cured and may also have differences in morphology and network structure.

An adhesive having a lower degree of cure due to early vitrification will, in turn, have a lower glass transition temperature (T_g) than an elevated temperature-cured system. In some cases, this T_g is close to the in-service operating conditions of these adhesives. Since the properties of a polymer are different below and above their T_g, it is possible that thermal, hydrolytic, and long-term mechanical properties, particularly under sustained loading and/or severe environments, could be greatly affected in service.

Most of the published literature has focused on elevated temperature-cure epoxy systems, and data on the properties of ambient temperature-cure systems are lacking. Since ambient temperature-cure adhesives are increasingly used in structural applications where exposure to sustained loads can occur, creep behavior (*i.e.*, permanent deformation under a constant sustained load) is particularly important. This study examines the properties of two ambient temperature-cure adhesives and explores the possibility of using dynamic mechanical testing, a common tool in polymer laboratories, to predict general trends in the creep behavior.

The thermo-viscoelastic and hygroscopic properties of two commercial, ambient temperature-cure structural epoxy adhesives were characterized using dynamic mechanical thermal analysis (DMTA), differential scanning calorimetry (DSC), thermogravimetric analysis (TGA), and moisture sorption analysis. Fourier transform infrared (FTIR) spectroscopy was employed to determine the extent of cure in the two epoxy systems. The long-term tensile creep compliance of the two systems was estimated by applying the Ninomiya and Ferry method to dynamic mechanical master curves generated using frequency-temperature superposition. Laboratory creep tests were also conducted on the two epoxy systems, and the results were compared with the creep compliance predicted from the dynamic mechanical data.

EXPERIMENTAL PROCEDURE[1]

Materials

The two commercial ambient temperature-cure epoxy structural adhesive systems used in this study were formulated by the same manufacturer and were purchased from a single commercial industrial supplier. The exact formulation of each adhesive was not known, and no attempt to de-formulate the systems was made; however, literature from the manufacturer indicates that these adhesives, hereinafter referred to as "Epoxy A" and "Epoxy B", have similar compositions but Epoxy A was formulated to have reduced cure times relative to Epoxy B. The Material Safety Data Sheets (MSDS) for the base resin in both Epoxies A and B listed a proprietary epoxy resin, calcium carbonate, and talc. The MSDSs indicated that the curing agent formulations for the two systems differed in that while both contained calcium carbonate and talc filler, Epoxy A contained aliphatic amines, benzyl alcohol, nonyl phenol, and phenol as major components, and Epoxy B contained aliphatic and cycloaliphatic amines, aromatic hydrocarbons, and benzyl alcohol. Phenols in general, and particularly nonyl phenol, are commonly used accelerators in epoxy adhesives [5].

[1]Certain commercial equipment, instruments, or materials are identified in this paper in order to specify the experimental procedure adequately. Such identification is not intended to imply recommendation or endorsement by the National Institute of Standards and Technology nor the Federal Highway Administration, nor is it intended to imply that the materials or equipment identified are necessarily the best available for this purpose.

Specimen Preparation

Analytical Measurements

Film specimens were prepared for use in DMTA, DSC, TGA, FTIR, and moisture sorption analysis. Using a double-cartridge manual caulk gun supplied by the adhesive manufacturer, the two components were ejected from their respective cartridges directly into a static-element mixing nozzle and deposited onto fluoropolymer-coated release paper. The deposited adhesive was drawn down into a uniform film using a steel draw-down bar with a 1.25-mm gap. Films were cured under laboratory conditions (nominally 21°C and 25% RH) for a minimum of 72 h before analysis. Cured film thicknesses ranged from 0.19 to 0.30 mm. In order to check reproducibility between lots, two separate packages of each adhesive system (manufactured at different times) were used to produce sets of specimens for testing. Similar properties were observed in the specimens produced from the different lots.

Creep Testing

Using the same double-cartridge manual caulk gun described above, the two components were ejected from the static-element mixing nozzle into 4.77-mm diameter plastic tubes. These tubes were filled with epoxy to a length of approximately 10 cm, and specimens were cured at ambient temperature in the tubes for a minimum of 24 h. The tubes were then carefully slit with a razor blade and peeled away from the cured adhesive, resulting in 4- to 5-mm diameter cylindrical specimens.

Post-Processing Exposure

Post-Curing

Due to anomalies that were observed during preliminary analysis, one set of Epoxy A film specimens was cured under ambient conditions as described earlier and then subjected to a 4 h post-cure at 60°C in a circulating air oven in an attempt to increase the extent of cure.

Moisture Saturation

Some samples of the Epoxies A and B films were exposed to a 22°C/100% RH environment to determine the effects of moisture sorption on their thermal and dynamic mechanical properties. This exposure consisted of suspending pre-cut film specimens over a reservoir of distilled water in a screw-top glass container for a minimum of 72 h and measuring their mass periodically until no

further increases in mass were observed. Dynamic mechanical thermal analysis (DMTA) was then carried out on the saturated specimens, taking care to minimize the time between the removal of the specimens from their container and the beginning of the analysis. One set of saturated specimens was dried under ambient conditions on the laboratory counter until their original dry mass was reached, and then analyzed *via* DMTA to determine whether the observed moisture effects were reversible.

Fourier Transform Infrared Spectroscopy (FTIR)

Infrared analysis of the cured epoxy films was carried out using a Nicolet Nexus FTIR spectrometer (West Palm Beach, FL, USA) equipped with a liquid nitrogen-cooled mercury-cadmium-telluride (MCT) detector and a SensIR Durascope (Smith Detection, Alcoa, TN, USA) attenuated total reflectance (ATR) accessory. Dry air was used as the purge gas. Consistent pressure on the films was applied using the force monitor on the Durascope. Three replicate spectra for each sample were recorded between 4000 and 600 cm^{-1} and were averaged over 128 scans. Standard uncertainties associated with this measurement are $\pm 1\,cm^{-1}$ in wavenumber and $\pm 1\%$ in peak intensity. In this report, spectra are presented in the range between 4000 and 800 cm^{-1}, due to detector limitations below 800 cm^{-1}.

Moisture Sorption Analysis

Moisture sorption isotherm measurements on Epoxies A and B films were carried out at $25 \pm 0.1^{\circ}C$ and relative humidity (RH) ranging from $\approx 0\%$ to 94% RH using a IGAsorp moisture sorption analyzer (Hiden Isochema, Warrington, UK) equipped with a microbalance having a mass resolution of 0.1 μg. The RH was raised in 10% RH increments from ≈ 0 to 94% RH. Before each moisture sorption experiment, the 0.3-mm thick specimens were dried in the analyzer at $25^{\circ}C$ and $\approx 0\%$ RH until essentially no mass loss (due to existing sorbed water) could be measured. The mass uptake (M_t) was recorded as a function of time until equilibrium sorption (M_∞) was obtained for each relative humidity. The relative changes in specimen mass were calculated with respect to the mass of the dried sample.

Moisture sorption kinetics of Epoxies A and B films were studied by generating sorption curves as a function of relative humidity at $25^{\circ}C$. For a thin film geometry in which diffusion from the edges is

negligible, the water uptake can be described by the following equation [6]:

$$\frac{M_t}{M_\infty} = 1 - \left[\frac{8}{\pi^2}\sum_{n=1}^{\infty}\frac{1}{(2n+1)^2}\cdot\exp\left(-D(2n+1)^2\pi^2\frac{t}{L^2}\right)\right], \quad (1)$$

where M_t is the mass of water sorbed at time t, M_∞ is the mass sorbed at the equilibrium, L is the film thickness, and D is the diffusion coefficient.

The diffusion coefficient can be determined from the initial slope of the plot of M_t/M_∞ as a function of $t^{1/2}/L$ for $M_t/M_\infty < 0.6$ using the reduced expression:

$$\frac{M_t}{M_\infty} = \frac{4}{L\sqrt{\pi}}\cdot\sqrt{Dt}. \quad (2)$$

Thermogravimetric Analysis (TGA)

TGA was carried out on a TA Instruments 2950 high resolution thermo-gravimetric analyzer (TA Instruments, New Castle, DE, USA). Specimens having a nominal mass between 15 and 20 mg were placed in ceramic sample pans. Samples were equilibrated at 25°C for 5 min, and then ramped to 500°C at 5°C/min. Analyses were carried out in a nitrogen atmosphere. The relative standard uncertainty in the mass measurements is typically ±0.1%, and the standard uncertainty in the temperature scale is typically ±0.1°C.

Differential Scanning Calorimetry (DSC)

Cured epoxy adhesives were sealed in aluminum pans and analyzed in a TA Instruments 2910 differential scanning calorimeter (New Castle, DE, USA) equipped with a refrigerated cooling system. Analysis was conducted in a nitrogen atmosphere in modulated DSC mode with a modulation frequency of ±1°C per 60 s. The initial mass loss onset temperature measured by TGA was used to establish the endpoint of the DSC experiments for each epoxy system. Samples were ramped from 0 to 60°C for Epoxy A, and from 0 to 95°C for Epoxy B, at a heating rate of 3°C/min, then cooled to 0°C at a rate of 3°C/min. This sequence was repeated in a second cycle. Subsequent analysis of Epoxy A to 90°C showed essentially no change in T_g following the heating and cooling cycles. The T_g was determined by the half-height method in the first heating curve and first cooling curve. The relative standard uncertainty in the heat flow measurements is typically

±3%, and the standard uncertainty in the temperature scale is typically ±0.2°C.

Dynamic Mechanical Thermal Analysis (DMTA)

Specimens were cut with a razor blade into 5.3- × 20-mm strips and tested in tensile mode on a Rheometrics Solids Analyzer (RSA) III (TA Instruments, New Castle, DE, USA). Specimens were consistently tightened in the instrument grips using a torque wrench set to 20 cN · m. In order to establish the linear viscoelastic (LVE) region of the epoxy systems, tensile strain sweeps were conducted between 0.001% and 1% strain at a test frequency of 10 Hz and at both room temperature (≈24°C) and 75°C. A tensile pre-load of 100 g was used to prevent the specimens from buckling. Because the samples tended to be brittle at room temperature, the majority of specimens failed at strains of ≤0.2% in the strain sweep experiments. The equipment has a feature that automatically increases the strain level at higher temperatures where the sample becomes softer to improve sensitivity in measuring the load. A test strain, which was initially set at 0.01% for low temperatures, reached a value of 0.04% at the highest temperatures. The strain sweep tests strongly suggest that these values are within the LVE domain.

DMTA temperature sweeps, which provide data on storage modulus (E′), loss modulus (E″), and tan delta, as a function of temperature, were carried out from 5 to 100°C, using a ramp rate of 5°C/min, frequency of 5 Hz, and tensile pre-load of 100 g. The dynamic mechanical glass transition temperature, T_g, was determined by taking the peak of the E″ curve, in accordance with ASTM E 1640-04 [7]. A minimum of three replicates were tested for each epoxy system. For the RSA III, the manufacturer-stated relative standard uncertainty in the force measurement is typically ±0.0002 g, and the standard uncertainty in the temperature scale is typically ±0.5°C.

Data for frequency-temperature superposition were generated by conducting combined temperature/frequency sweeps from 0.005 to 10 Hz using five different frequencies in each decade, and from 20 to 90°C at intervals of 3°C.

Creep Testing

Creep experiments were performed on the cylindrical samples using a Dynastat mechanical spectrometer run in load control (IMASS, Hingham, MA, USA). Specimens were approximately 10 cm in length and gripped to produce a gage length of about 7 cm. This length was

selected to help minimize grip effects and to maximize sensitivity for small creep displacements. Experiments were performed at 5°C temperature intervals from 20 to 80°C. Following load application, specimen displacement was recorded from 0.01 to 1000 s at 10 points per decade. Depending on sample and machine settings, between 20 and 50 ms were required to apply the load so to avoid transients associated with the loading step; data obtained at times less than 0.2 or 0.5 s were not included in the analysis. The initial stress level was 1.2 MPa (2.0 kg load) but, as the temperature increased, the load was reduced to minimize strain levels (final value 0.2 MPa, 0.4 kg). Creep strains ranged from 0.003 to 0.8%. The higher values, which were reached at the higher temperatures, are larger than those used in the dynamic tests, but based on the DMTA strain sweep experiments, are probably within the linear viscoelastic regime. A recovery period of at least 5400 s was allowed after a new temperature was reached in each temperature step. By conducting the experiments with increasing temperatures, the recovery process should be accelerated. The standard uncertainty in the load measurement was ±0.1 g. For displacement, the standard uncertainty was ±0.00005 mm at all but the highest temperatures where it was ±0.0005 mm. The resulting data were analyzed for the applicability of time-temperature superposition, and creep master curves were generated.

Frequency-Temperature or Time-Temperature Superposition

The dynamic mechanical data were analyzed for the applicability of frequency-temperature superposition. A software program developed previously by Hunston *et al.* [8] was used to transform E′ and tan delta data from DMTA temperature/frequency sweeps into E′, E″, and tan delta master curves as a function of frequency. Tan delta and E′ curves at each temperature were shifted horizontally along the frequency axis with respect to data at the previous temperature to obtain the best visual overlap of the tan delta data. A small vertical shift was then applied, if needed, to achieve the optimum overlap of the E′ curves. A reference temperature was then selected and the data were re-normalized to that temperature. The program also has the capability to take the dynamic mechanical master curves (modulus *vs* frequency) and predict the creep behavior (creep compliance *vs* time) using the approximation of Ninomiya and Ferry [9].

This same computer program can be applied to the experimentally generated creep data. The difference here is that the independent variable is time rather than frequency. The creep compliance curves

at different temperatures are shifted interactively until the best visual overlap is obtained. This permits the applicability of time-temperature superposition to be tested, and master curves to be generated for creep compliance.

RESULTS AND DISCUSSION

FTIR Analysis

The FTIR spectra of as-processed Epoxies A and B are compared in Fig. 1. The spectrum of Epoxy A showed a small peak at 911 cm^{-1}

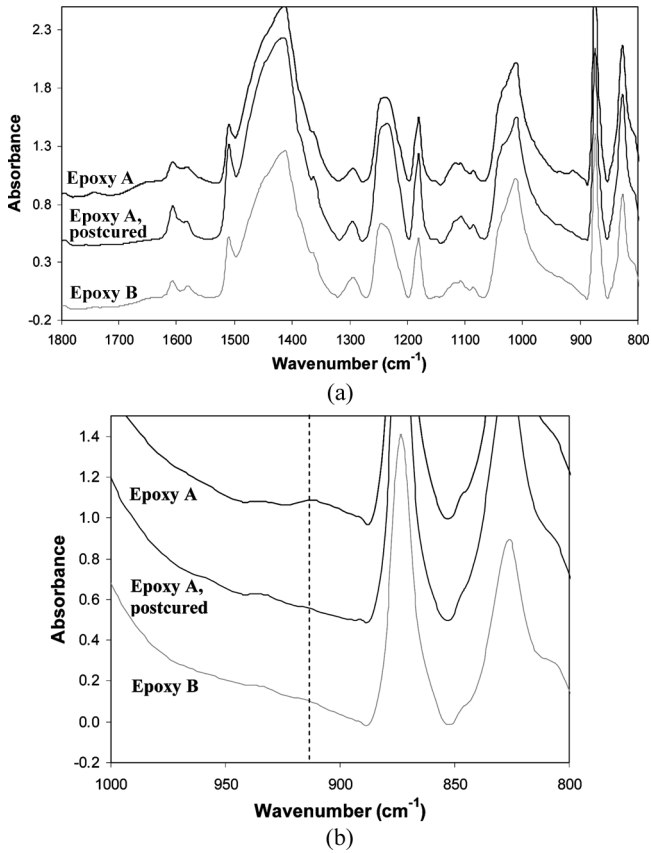

FIGURE 1 FTIR spectra of Epoxy A, Epoxy A post-cured, and Epoxy B, showing location of epoxide ring peak at 911 cm^{-1} (dashed line). (a) 800 to 1800 cm^{-1} region and (b) 800 to 1000 cm^{-1} region.

corresponding to the epoxide ring, indicating that it contained unreacted epoxide functional groups. No epoxide ring peak was visible in the spectrum of Epoxy B. This observation suggests that, assuming that the two systems have similar base resin/curing agent stoichiometry, Epoxy A had a lower degree of cure than Epoxy B when processed under ambient conditions as recommended by the manufacturer. Also contained in Fig. 1 is the FTIR spectrum of Epoxy A following postcuring at 60°C for 4 h. In this spectrum, the epoxide ring peak is no longer visible, indicating that elevated temperature treatment increased the degree of cure. Figure 1(b) is an expansion of Fig. 1(a) in the 800 to 1000 cm^{-1} region for ease of comparison.

Thermal Analysis

As-Processed Specimens

The T_g of a crosslinked network is an important material property that is correlated with the extent of cure or crosslinking [10]. Glass transition temperatures of the cured systems were measured using both DSC and DMTA; TGA was utilized to assess the overall thermal stability of the cured systems. Table 1 summarizes data from DSC, TGA, and DMTA for both materials.

Figure 2 shows representative TGA curves for Epoxies A and B. For Epoxy A, the onset of initial mass loss occurred at 75°C, compared with 115°C for Epoxy B. These temperatures are far below the temperatures needed to disrupt most organic bonds; thus, the mass loss is most likely attributed to the volatilization of low-molecular weight, non-network components. The lower onset temperature for Epoxy A may be attributed to the presence of accelerator and/or the different curing agents used. The primary decomposition event involving

TABLE 1 Summary of Thermal Analysis Data for Epoxy A and Epoxy B, Obtained from Differential Scanning Calorimetry (DSC), Dynamic Mechanical Thermal Analysis (DMTA), and Thermogravimetric Analysis (TGA)

Temperature (°C)	Epoxy A	Epoxy B
DSC		
First heat T_g	48.3 ± 1.3	54.9 ± 1.0
First cool T_g	41.5 ± 2.0	53.5 ± 0.3
Second heat T_g	43.6 ± 2.7	53.8 ± 2.1
Second cool T_g	41.3 ± 2.8	53.3 ± 0.3
DMTA T_g (E″ peak)	50.3 ± 1.5	52.2 ± 0.9
TGA – onset of mass loss	75 ± 1.2	115 ± 1.0

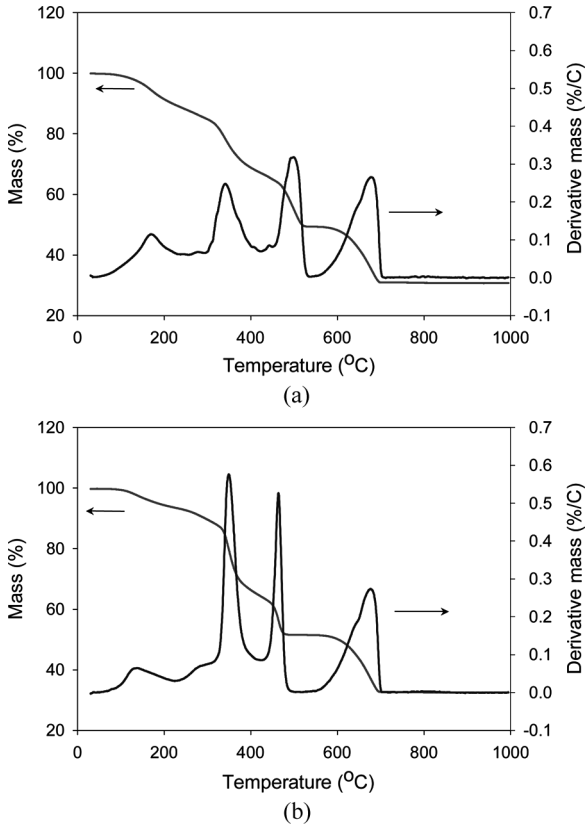

FIGURE 2 Representative TGA curves for (a) Epoxy A and (b) Epoxy B, showing mass loss curve and derivative curve for residual mass as a function of temperature.

breakage of common bonds found in organic molecules (carbon-carbon, carbon-oxygen, carbon-nitrogen) occurred between 340 and 350°C for both systems. The initial mass loss onset temperature was used to establish the endpoint of the DSC experiments for each epoxy system.

Representative modulated DSC reversing heat flow curves are shown in Fig. 3. As typically seen for filled thermoset polymers, the DSC transitions are shallow, but the T_g of the resin could still be determined. The first heat T_g of Epoxy B (54.9°C) was observed to be slightly higher than that of Epoxy A (48.3°C). During the subsequent cooling step, Epoxy A exhibited a small but reproducible decrease in T_g to 41.5°C, with no additional changes in T_g observed in the second heating and cooling cycles. No changes in the T_g of Epoxy

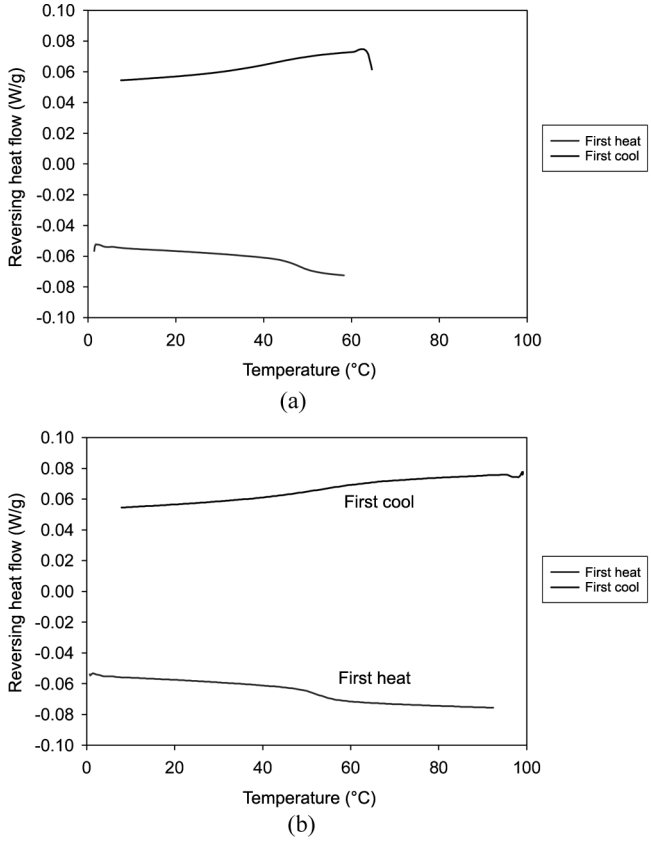

FIGURE 3 Representative modulated DSC curves for (a) Epoxy A and (b) Epoxy B, showing reversing heat flow for the first heating and cooling cycles.

B were observed following either the first or second heating/cooling cycles.

Changes in T_g of thermoset materials during DSC analysis can occur following the first heating cycle, and are attributed to thermal post-curing [10]. This phenomenon is not unexpected for this system, which was observed to contain a small amount of unreacted functional groups as seen in the FTIR analysis presented earlier. If the material is exposed to temperatures above T_g, the mobility of the reactive groups is restored and crosslinking can continue, sometimes evidenced by the appearance of a residual cure exotherm in the DSC curve. No such exothermic peaks were observed in the DSC analysis of Epoxy A; however, it is possible that the amount of heat released was very

small and the exotherm intensity fell below the resolution of the instrument. Nevertheless, in the great majority of cases, the T_g of the post-cured material shifts towards *higher* temperature, not *lower*, as observed in this study for Epoxy A.

Moisture Sorption Analysis

Moisture sorption experiments on as-processed Epoxies A and B specimens were carried out at 25°C for a range of relative humidities between ≈0 and 94% RH. In Fig. 4, the sorption isotherms are expressed in mass uptake with respect to the mass of the dried specimens. Over the entire range of relative humidity studied, Epoxy A exhibited a higher overall moisture uptake than Epoxy B. Between 0 and 50% RH, the mass uptake for both epoxies increased linearly with increasing relative humidity. Above 50% RH, sorption isotherms of both epoxies show a significant upturn. Above 80% RH, the upturn in the sorption isotherm for Epoxy B became more pronounced while the sorption isotherm of Epoxy A exhibited a decrease in slope. After prolonged exposure, the mass uptake in Epoxy A at both 90% and 94% RH decreased, as shown in Fig. 5.

Epoxies A and B are assumed to contain similar amounts of calcium carbonate and talc filler and, thus, the filler contribution to moisture

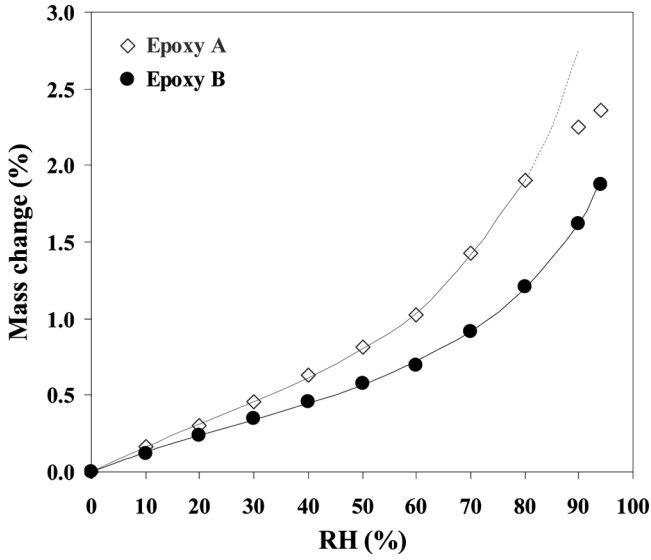

FIGURE 4 Water sorption isotherms of Epoxies A and B at 25°C.

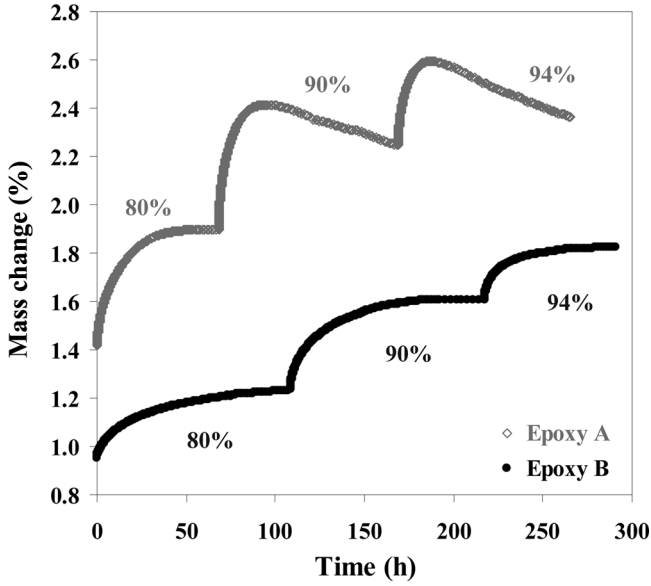

FIGURE 5 Adsorption curves of Epoxies A and B at 80, 90, and 94% RH at 25°C.

uptake should be similar. TGA analysis of residual mass (Fig. 2) shows that both materials contained approximately 30 mass % filler. As previously discussed, FTIR analysis of as-processed Epoxy A films showed that it was not fully cured and contained unreacted epoxy functional groups. Since the ring-opening reaction of epoxide groups produces secondary hydroxyls, it could be inferred that the concentration of polar hydroxyl groups in Epoxy A available to form hydrogen bonds with water molecules is lower than that of Epoxy B. Consequently, the greater amount of sorbed moisture in Epoxy A cannot be attributed to the concentration of chemical groups associated with the curing of epoxies. A more reasonable hypothesis may be that the different sorption behaviors of Epoxies A and B are due to the presence of accelerators which could affect the composition and microstructure of Epoxy A.

Figure 5 displays moisture sorption curves for 80, 90, and 94% RH as a function of time for both Epoxies A and B. The sorption curves of Epoxy B exhibited an initial moisture uptake stage followed by equilibrium. On the other hand, Epoxy A exhibited rapid moisture uptake followed by mass loss. Later results will show a depression in T_g for moisture-saturated Epoxies A and B specimens, which confirms that

some degree of plasticization was induced by sorbed water molecules. As will be seen, the T_g of moisture-saturated Epoxy A was below the temperature at which the moisture sorption experiment was conducted so the material was in the rubbery state during the experiment. It can be speculated that the mass loss observed for Epoxy A is attributed to the loss of low-molecular mass components trapped in the epoxy film after vitrification but released when moisture swells the network. This postulation is supported by Fig. 5, which shows higher mass loss at 90 and 94% RH than at 80% RH. At these relative humidity levels, water was likely condensed and enabled the migration of low molecular mass componentsout of the epoxy.

In addition, the positive deviation from linearity of the isotherm shown in Fig. 4 above 60% RH is commonly explained by the plasticization of the epoxy resin by water, resulting in an increase in chain mobility, and subsequently, the diffusion coefficient, D [11]. The diffusion coefficients of water for Epoxies A and B at 25°C, calculated *via* Eq. (2), as a function of the relative humidities, are shown in Fig. 6. The diffusion coefficients for Epoxy B ranged from 1.91×10^{-10} to 5.50×10^{-10} cm^2/s, and exhibited a slight decrease with increasing relative humidity. On the other hand, the diffusion coefficient for Epoxy A is relatively constant for RH < 60%, but at RH > 60%, D increases with increasing relative humidity.

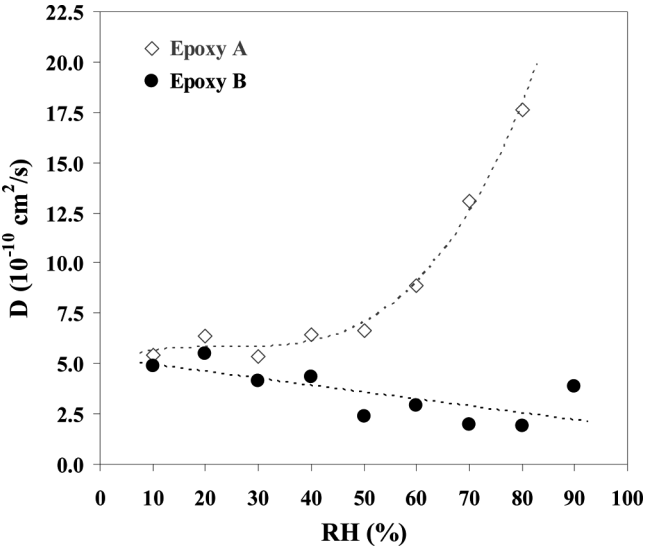

FIGURE 6 Moisture diffusion coefficients at 25°C of Epoxies A and B as a function of relative humidity.

Dynamic Mechanical Thermal Analysis

As-Processed Specimens

Figure 7 shows representative E′, E″, and tan delta curves at 5 Hz as a function of temperature for Epoxies A and B. The E′ curve distinctly shows the three regions of viscoelastic behavior—glassy, transition, and rubbery—that are characteristic of crosslinked amorphous polymers. As measured by the peak of the E″ curve, the dynamic mechanical T_gs of Epoxies A and B were 50.3 and 52.5°C, respectively.

The average storage moduli of Epoxies A and B at 30°C were similar at 5.21 ± 1.25 and $5.84\,\text{GPa} \pm 1.23\,\text{GPa}$, respectively, as would be

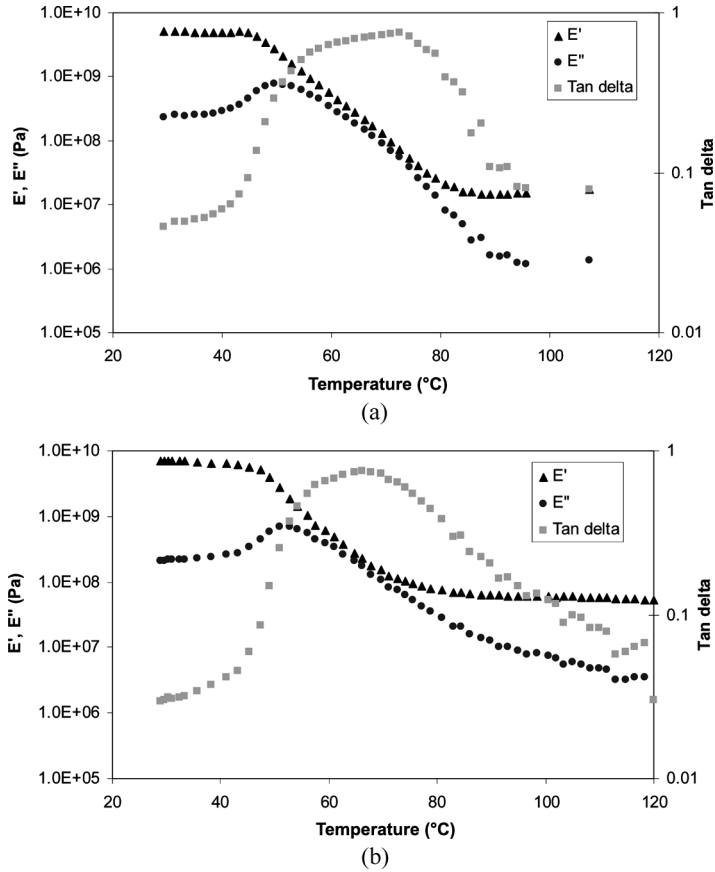

FIGURE 7 Representative E′, E″, and tan delta curves for (a) Epoxy A and (b) Epoxy B, obtained at 5 Hz and strains $\leq 0.04\%$.

expected for polymeric materials in their glassy state. However, the rubbery portion of the storage modulus measured at 100°C for Epoxy A was approximately 10 MPa while that of Epoxy B was 46 MPa. The lower rubbery modulus of Epoxy A could be attributed to factors such as lower crosslink density or lower filler content and would be expected to influence long term creep behavior. It was also noted that for both materials, the width of the E′, E″, and tan delta transitions were greater than those typically observed for simple model epoxies [8]. The width of the tan delta peak for Epoxy A is somewhat broader than that for Epoxy B; in fact, the shape of the tan delta peak for Epoxy A suggests the possibility of two overlapping peaks. The broader transitions indicate that both epoxies are more complex and heterogeneous than simple thermosets; therefore, there is a broader range of response times for the molecular motions associated with the glass transition. This can occur when a system contains a mixture of different base resins and/or curing agents, giving rise to complex or multiple network structures. If the components are significantly different and distinct from each other, separate transition peaks are seen. If the components are similar but distinct, the peaks can overlap creating a broadened transition with contributions from each component [12]. Fillers that interact chemically or physically with the resin can produce a similar result: in a review of pigment effects on coating properties [13], the width of the tan delta peak was reported to be greater for a pigment-filled coating relative to its non-filled counterpart. Therefore, the presence of the inorganic fillers in the epoxy systems could contribute to the breadth of the tan delta peaks observed in this study.

Post-Cured Specimens

As discussed earlier, Epoxy A may have vitrified early in the curing process and remained undercured, possibly due to the presence of accelerators that decreased its cure time. To follow up on this possibility, DMTA temperature sweeps were carried out after specimens were post-cured at 60°C for 4 h. This temperature was chosen for post-curing because it is above the T_g but below the onset of mass loss observed *via* TGA. As seen in Fig. 8, a decrease in the T_g (peak of E″ curve) following post-cure is observed, similar to the decrease in T_g following the first heating cycle in the DSC analysis. As discussed earlier, this behavior is unusual in that most elevated temperature post-curing operations tend to initiate additional polymerization or crosslinking in the network, which, in turn, increases the T_g. At the present time, the reasons for this unexpected behavior are not understood and speculations will be avoided, particularly in the light of the

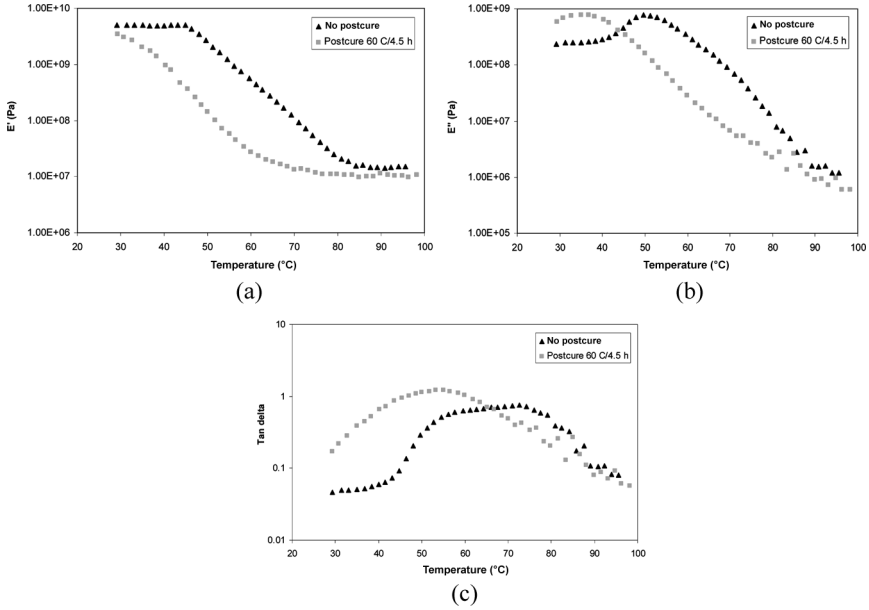

FIGURE 8 (a) E′, (b) E″, and (c) tan delta curves for Epoxy A prior to and following elevated temperature postcure, obtained at 5 Hz and strains $\leq$0.04%.

proprietary nature of the epoxy formulations. The behavior of specimens post-cured at higher temperatures was not investigated, and could differ from the specimens post-cured at 60°C.

Moisture-Saturated Specimens

DMTA analyses of saturated Epoxies A and B exposed to a 23°C/100% RH environment are shown in Figs. 9 and 10, respectively. Test specimens were flexible and rubbery following exposure to a high relative humidity environment, in contrast to the brittleness of the as-prepared specimens. The T_g of Epoxy A decreased to 15°C following moisture exposure; upon drying of the saturated specimens, the original T_g of 50°C was recovered. Epoxy B also exhibited a decrease in T_g from 50 to 32°C when saturated. After drying, a slightly higher T_g of 57°C was observed; this was higher than the T_g that was previously measured for the dry material. The glassy modulus of the two epoxy systems was also observed to decrease when saturated, due to swelling and plasticization by absorbed moisture. In the case of Epoxy B, the original glassy modulus was mostly recovered when the specimens were dried, whereas, for Epoxy A, the glassy modulus

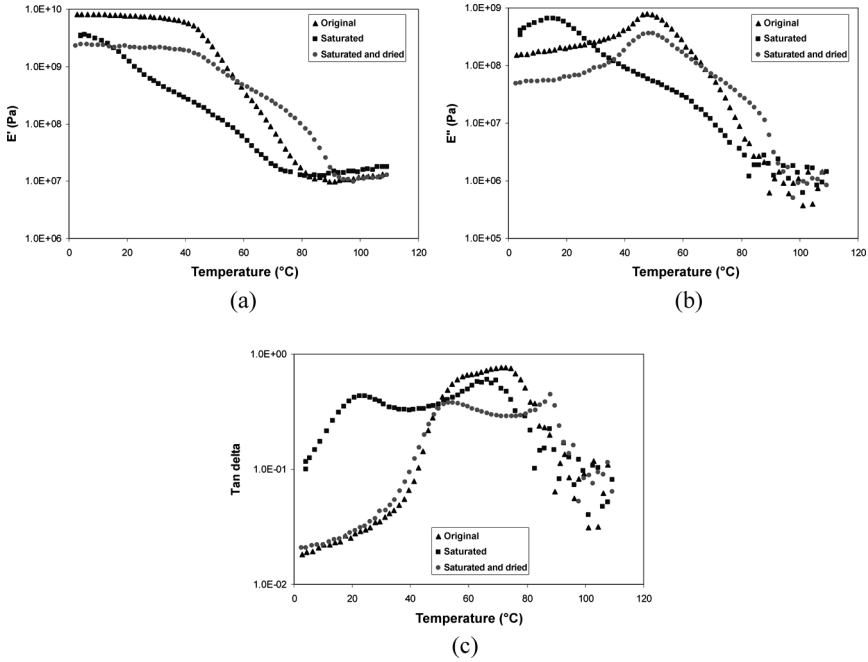

FIGURE 9 Comparison of (a) E′, (b) E″, and (c) tan delta curves for Epoxy A prior to moisture saturation, following saturation, and following saturation and drying, obtained at 5 Hz and strains $\leq$0.04%.

for the specimens that were saturated and dried was lower than the original modulus.

As observed in Figs. 9(c) and 10(c), the tan delta curves for the saturated epoxies also exhibited interesting characteristics. Both systems initially showed a broad tan delta peak when dry that resolved into two separate peaks when saturated. After drying, two separate tan delta peaks were still observed, even though the T_gs had reverted back to their original dry values. If the large breadth of the tan delta peak suggests a heterogeneous structure, then it is possible that different components of that structure interact with water in different ways. Without a knowledge of composition or morphology, one can only speculate, but it has been documented by other researchers that cured epoxies have heterogeneous, phase-separated structures, consisting of hard, highly crosslinked phases and low molecular mass, less crosslinked phases [14,15]. The most common examples are multicomponent materials or systems where inadequate mixing produces an uneven distribution of curing agent and/or accelerator. The

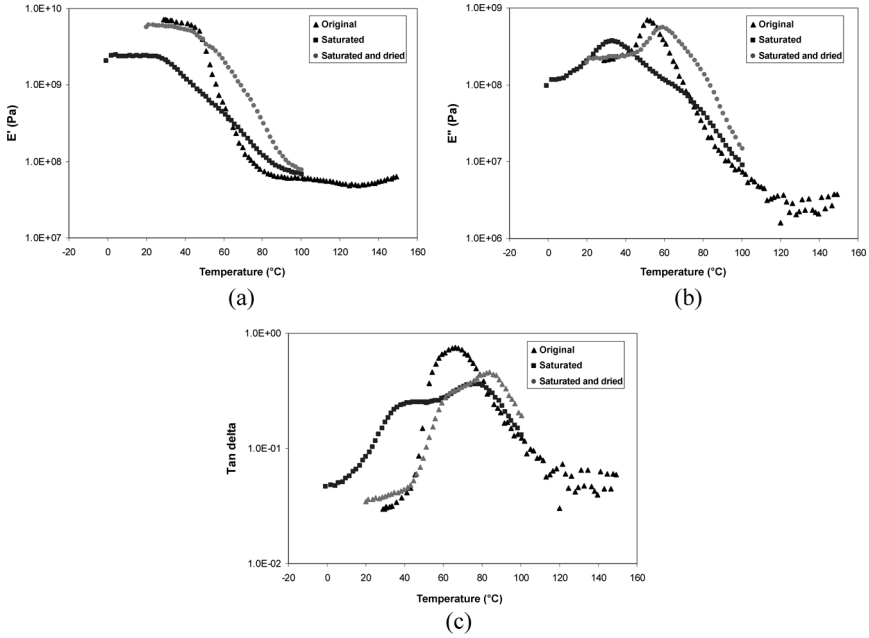

FIGURE 10 Comparison of (a) E′, (b) E″, and (c) tan delta curves for Epoxy B prior to moisture saturation, following saturation, and following saturation and drying, obtained at 5 Hz and strain $\leq 0.04\%$.

sorption of water may perturb one phase but not the other. Another possibility is that the absorbed moisture plasticizes the resin and increases local mobility, thus allowing additional phase separation of the different components to occur. The peaks corresponding to the components would become more distinct and such changes may persist after the water is removed. In any case, it is evident that the effects of moisture were not fully reversible upon desorption within the time scale studied here, and that changes in the polymer network structure had occurred due to moisture sorption.

Temperature/frequency sweeps, which typically take >9 h to complete, were not carried out on the saturated materials. The loss of moisture that would occur throughout the test would cause the viscoelastic properties of the material to continually change, compromising the quality of data and making it difficult to construct master curves. However, based on prior knowledge of the effects of moisture on the mechanical properties of glassy polymers, it is probable that the creep behavior observed in the dry specimens would be accentuated in the

presence of moisture. Feng *et al.* have shown the equivalence between temperature and moisture in the creep behavior of a model epoxy system by observing a similar viscoelastic response at a higher temperature when dry and at a lower temperature when saturated [16]. This showed that the presence of sorbed moisture can initiate creep response similar to that observed under dry, elevated temperature conditions.

Frequency-Temperature Superposition of Dynamic Data

The principle of frequency-temperature superposition [17] is based on the hypothesis that, for a viscoelastic material, changing the temperature in an experiment produces the same effect as shifting the frequency range over which the measurements are made. This relationship can be exploited by conducting tests at a variety of temperatures and frequencies and shifting the results until they superimpose, thus generating a master curve that predicts behavior over a wide range of frequencies. If this relationship holds, the material is called *thermo-rheologically simple*. No multicomponent material is truly thermo-rheologically simple, but this model is a good approximation for many simple polymers. For thermosets, superposition has been shown to work well for an epoxy with a simple chemistry, but for more complex formulations such as those often used in commercial materials, superposition may provide only a fair approximation or even yield completely misleading results [8]. The usual explanation for deviations from simple behavior is that formulations that are mixtures of base resins and curing agents generate complex structures in the cured material. Unless all components in the system have the same temperature dependence, perfect superposition is not obtained. As the differences in temperature dependence of the various components increases, the quality of the superposition decreases and the predictions of long-term behavior become less reliable.

Figures 11(a, b) and 12(a, b) show the dynamic mechanical master curves for Epoxies A and B, respectively, representing the predictions of E', E'', and tan delta over an extended frequency range. Neither epoxy system was truly thermo-rheologically simple, with Epoxy A showing more deviation from simple behavior than Epoxy B. This is particularly evident in the tan delta curves which seemed to be the most sensitive to the quality of superposition.

Figures 11(c) and 12(c) show horizontal shift factor plots that indicate how much the data at each temperature must be shifted to obtain superposition. At temperatures well above the T_g, shift factor plots are normally concave upward, displaying behavior described by the

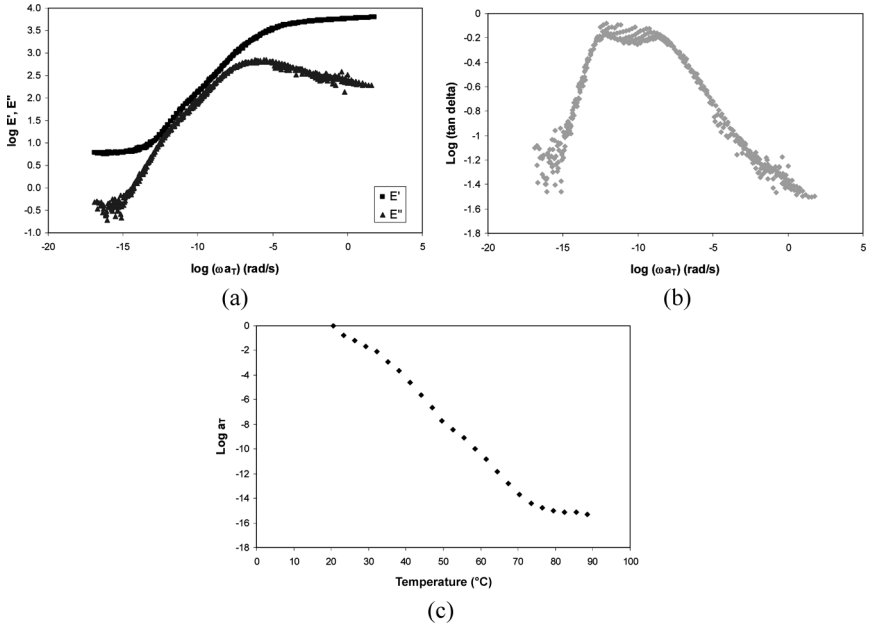

FIGURE 11 (a) E′ and E″ master curves, (b) tan delta master curve, and (c) shift factor plot for Epoxy A, obtained from frequency-temperature sweeps at strains $\leq$0.04%, referenced to 20°C.

well-known Williams-Landel-Ferry (WLF) equation [18], while below T_g, the plots are concave downward due to the so-called physical aging effect [8]. The plots in Figs. 11(c) and 12(c) show some tendency toward this behavior but have a more complicated structure. This is particularly evident with Epoxy A where the curve appeared to have two transitions. This is consistent with the suggestion of a double peak in the tan delta curve.

Despite the deviations from thermo-rheologically simple behavior shown in Figs. 11 and 12, further analysis may be able to provide information on general trends. Because the creep behavior of these materials is of interest, the creep compliance curves for the two epoxies were calculated and shown in Fig. 13. A reference temperature of 51.25°C was selected since this is the average T_g for the two epoxies. In light of the discussion above, this is in no way a substitute for the direct measurement of creep behavior; however, it is useful in determining the appropriate test conditions for measuring creep and identifying behavior of interest. Since the materials show significant deviations from thermo-rheologically simple behavior, small differences

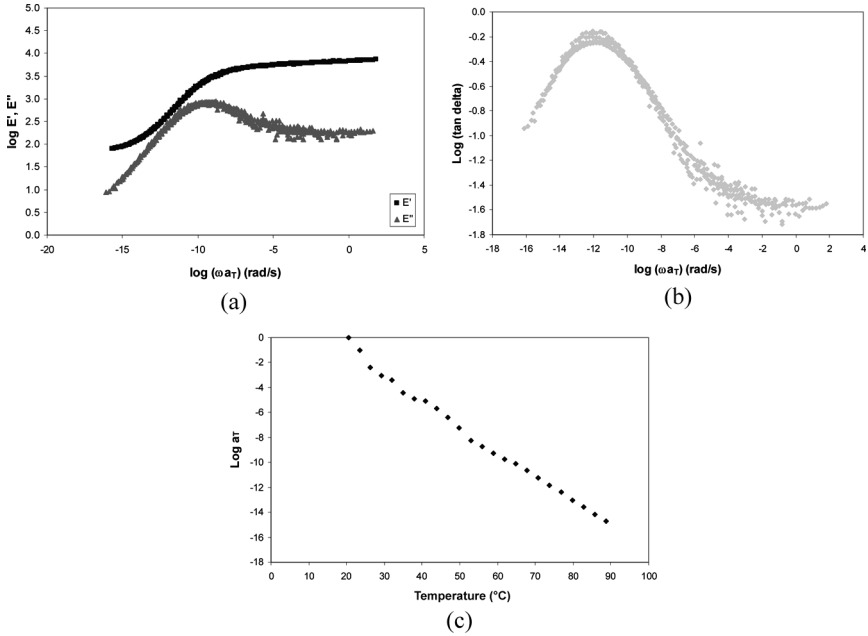

FIGURE 12 (a) E′ and E″ master curves, (b) tan delta master curve, and (c) shift factor plot for Epoxy B, obtained from frequency-temperature sweeps at strains $\leq$0.04%, referenced to 20°C.

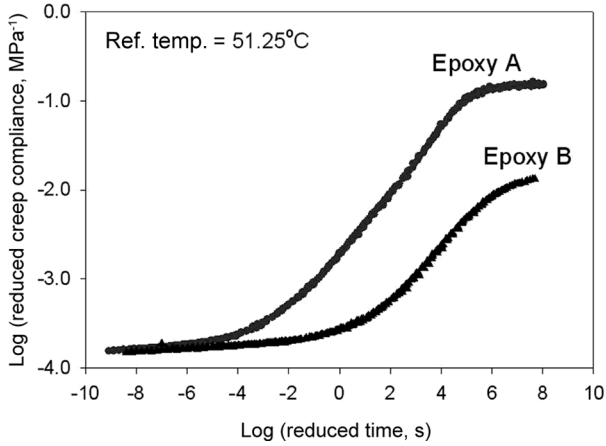

FIGURE 13 Comparison of estimated creep compliance for Epoxies A and B, referenced to 51.25°C, obtained from frequency-temperature sweeps at strains $\leq$0.04%.

in predicted response would not be significant. However, the differences seen in Fig. 13 are substantial. The short time creep responses look similar but the difference between the curves increases with time, and eventually the predicted creep compliance of Epoxy A significantly exceeds that of Epoxy B.

The large difference in predicted creep is somewhat unexpected since the differences observed in T_g and the width of the glass to rubber transition are relatively small. The rubbery plateau modulus of Epoxy A was significantly lower than that for Epoxy B, and this would affect long-term behavior, but the creep curves were quite different even at moderate times. Consequently, it is of interest to test the prediction by examining the results from actual creep tests.

Time-Temperature Superposition of Creep Data

Figure 14 shows the results of applying time-temperature superposition to the experimentally measured creep data for Epoxies A and B at a reference temperature of 51.25°C. The curves for different temperatures superimposed quite well so the results can be compared with Fig. 13. There are some differences observed between the two sets of curves. A number of factors could contribute to these differences. The strain levels were not the same, but this should not be a factor since both experiments are expected to be in the linear viscoelastic

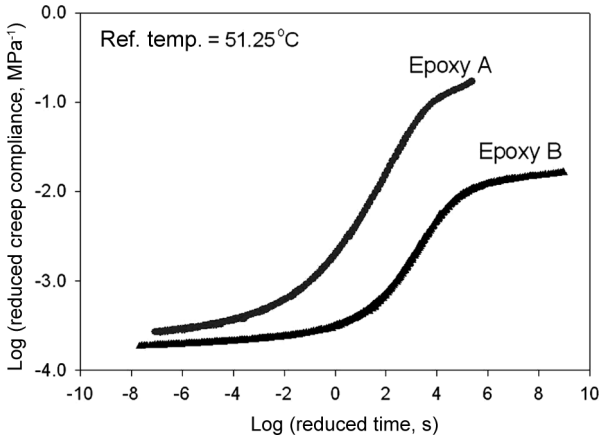

FIGURE 14 Comparison of creep compliance master curves for Epoxies A and B referenced to 51.25°C, obtained from superposition of creep curves at temperatures from 25 to 80°C.

range. On the other hand, two different instruments were used, and there can be some difference in data from two instruments even when both are carefully calibrated. In addition, the sample length in the dynamic mechanical experiments was quite short, potentially leading to grip effects that were not present in the creep tests. Because the creep experiments require two to three times as long to complete, the thermal histories were significantly different for the two experiments. Finally, the sample geometry may have affected the curing process. The dynamic tests utilized very thin samples so the exothermic reaction produced relatively little heating. The creep samples, on the other hand, were 4 to 5 mm in diameter so significant heating may have occurred during fabrication.

While each of these factors was small, the sum of the differences could be enough to shift the predicted and measured creep data away from each other. Despite these differences, the general trends in the data from the two experiments were quite similar. In both cases, Epoxy A exhibited more creep than Epoxy B, and the transition for Epoxy A started at much shorter times. Consequently, the general predictions from the dynamic mechanical tests appear to be valid.

The question of why materials with a moderate difference in rubbery plateau moduli and small differences in T_g and transition width have such large differences in creep behavior still remains unanswered. The explanation could lie in the fact that since all three of these factors contribute to increased creep in Epoxy A, their combination produces a large effect even though individually their effects are expected to be small.

SUMMARY AND CONCLUSIONS

The thermo-viscoelastic properties, including dynamic and creep responses, of two commercial, ambient temperature-cure epoxy structural adhesives used in construction applications were analyzed and compared. The adhesives were formulated by the same manufacturer and were chemically similar, but one system (Epoxy A) was formulated with accelerators to shorten its cure time.

Our results indicated that, although Epoxy A was formulated to be cured at ambient temperature, it appeared to be under-cured when processed under these conditions in the laboratory. FTIR analysis revealed the presence of residual epoxide in Epoxy A, which disappeared following elevated temperature post-curing; no such peak was observed in the FTIR analysis of Epoxy B. Onset of mass loss occurred at a lower temperature for Epoxy A as compared with Epoxy B. This mass loss could be attributed to the presence of

non-reacted or non-network chemical species that are volatile or easily removed. It is hypothesized that the presence of these species is related to the accelerator, which is present in Epoxy A but not in Epoxy B, and/or to the differences in curing agent formulation.

T_g depression and appearance of additional or more distinct transitions in E′, E″, and tan delta were observed in both epoxy systems following moisture saturation. The saturated T_g of Epoxy A was below room temperature, making it a rubbery material under ambient conditions, whereas the saturated T_g of Epoxy B was above room temperature. Moisture sorption experiments at 25°C showed that Epoxy A exhibited higher moisture uptake than Epoxy B over the entire range of humidities studied, with Epoxy A also exhibiting mass loss after prolonged high humidity exposures. The resulting increase in chain mobility led to an increase in moisture diffusion coefficient with increasing relative humidity for Epoxy A. The observed mass loss could be due to the desorption of low molecular mass, water-soluble components trapped in the vitrified resin.

In DMTA temperature sweeps, both epoxies showed broad transitions although Epoxy A was somewhat broader with the suggestion of two overlapping transitions. This indicates that Epoxy A had a more complex and heterogeneous structure than Epoxy B. Another difference is that while the glassy moduli of the two systems were similar, Epoxy A had a significantly lower rubbery plateau modulus than Epoxy B, which could potentially exacerbate long-term creep.

Temperature/frequency sweeps were carried out to examine the applicability of frequency-temperature superposition. Neither of the epoxies was truly thermo-rheologically simple, with Epoxy A exhibiting more deviation from simple behavior than Epoxy B. Nevertheless, the master curves were used to estimate creep compliance for the two epoxies. Although not a substitute for the direct measurement of creep, the creep compliance curves generated from frequency-temperature superposition data indicated the general trends in behavior that might be expected. The results suggested that Epoxy A will exhibit significantly more creep than Epoxy B. These predictions were tested by direct creep measurements. Although there were differences between the creep results and the predictions from the dynamic mechanical tests, the major prediction that Epoxy A is much more susceptible to creep than Epoxy B was confirmed.

This large difference in creep behavior for two systems that had similar chemistry and short-term properties can be attributed to the fact that the small differences in T_g and the width of the glass to rubber transition combine with a significant difference in the rubbery plateau moduli to produce increased creep in Epoxy A. Consequently,

it is important to examine long term behavior as well as short term properties when selecting an adhesive for applications that require long-term durability. In this connection, the results suggest that dynamic mechanical testing and frequency-temperature superposition can provide a useful screening technique for many polymeric systems.

REFERENCES

[1] Cook, R. A. and Konz, R. C., *ACI Structural Journal* **98**, 76–86 (2001).
[2] Karbhari, V. M., Engineer, M., and Eckel II, D. A., *J. Mater. Sci.* **21**, 147–156 (1997).
[3] Steckel, G. L., Hawkins, G. F., and Bauer, J. L., *Proceedings of the 2nd International Conference on Composites in Infrastructure*, H. Saadatmanesh and M. R. Ehsani (Eds.) (Tuscon, AZ, 1998), pp. 460–475.
[4] Gillham, J. K. and Enns, J. B., *Trends in Poly. Sci.* **2** (12), 406–418 (1994).
[5] Behm, D. T. and Gannon, J., *Engineered Materials Handbook, Vol. 3: Adhesive and Sealants*, (ASM International, Novelty, OH, USA, 1990), pp. 94–102.
[6] Comyn, J., *Polymer Permeability*, (Elsevier Applied Science, London, UK, 1985).
[7] ASTM E1640-04, Standard Test Method for Assignment of the Glass Transition Temperature by Dynamic Mechanical Analysis. ASTM International, West Conshocken, PA, 2009.
[8] Hunston, D. L., Carter, W., and Rushford, J. L., *Developments in Adhesives – 2*, A. J. Kinloch (Ed.) (Applied Science Publishers Ltd., London, 1980), pp. 125–172.
[9] Ninomiya, K. and Ferry, J. D., *J. Colloid Sci.* **14**, 36–48 (1959).
[10] Farifa, S. and Bouazzi, A., *J. Thermal Analysis* **48**, 297–307 (1997).
[11] Crank, J. and Park, G. S., *Diffusion in Polymers*, (Academic Press, London, 1968).
[12] Cohen, R. E. and Ramos, A. R., *Macromolecules* **12** (1), 131–134 (1979).
[13] Perari, D. Y., *Prog. Org. Coatings* **50**, 247–263 (2004).
[14] VanLandingham, M. R., Eduljee, R. F., and Gillespie, J. W., *J. Appl. Polym. Sci.* **71**, 787–798 (1999).
[15] Cuthrell, R. E., *J. Appl. Polym. Sci.* **12**, 1263–1278 (1968).
[16] Feng, C.-W., Keong, C.-W., Hsueh, Y.-P., Wang, Y.-Y., and Shue, H.-J., *Int. J. Adhes. Adhes.* **25**, 427–436 (2005).
[17] Ferry, J. D., *Viscoelastic Properties of Polymers*, (John Wiley and Sons, New York, 1980).
[18] Williams, M. L., Landel, R. F., and Ferry, J. D., *J. Amer. Chem. Soc.* **77**, 3701–3706 (1955).